Physica 127B (1984) 422–425
North-Holland, Amsterdam

TRANSPORT OF VERY-HIGH-FREQUENCY PHONONS GENERATED BY METALLIC POINT CONTACTS IN RUBY

R.J.G. GOOSSENS, J.I. DIJKHUIS and H.W. DE WIJN
Fysisch Laboratorium, Rijksuniversiteit, P.O. Box 80.000, 3508 TA Utrecht, The Netherlands

A.G.M. JANSEN and P. WYDER
Research Institute for Materials, University of Nijmegen, Toernooiveld, 6525 ED Nijmegen, The Netherlands

With a novel technique point contacts are used for the generation of very-high-frequency phonons in ruby. In an optical experiment selective for near-zone-boundary phonons, the injected phonons are observed by the R_2 fluorescence from a small zone prepared by pulsed optical pumping at distances up to 0.6 mm from the contact. In a time of flight experiment phonons injected in Al_2O_3 are detected in a broad band with a superconducting tin film.

We first present a novel technique of injecting very-high-frequency acoustical phonons in insulating crystals at low temperatures, and subsequently show that such phonons may travel over macroscopic distances. The technique of generation is based on a metallic point contact, which allows phonon production in very small volumes by dissipation of electrical current [1, 2]. The detection in the insulator has been accomplished, at various positions in the crystal, by the phonon-induced enhancement of a suitable luminescence transition of an optically pumped center. Such a scheme is under appropriate circumstances selective to phonons near the Brillouin-zone boundary of the crystals. As an example we have taken ~500 ppm ruby (Cr^{3+}: Al_2O_3). We have also observed both longitudinal and transverse phonons to traverse a crystal of sapphire (Al_2O_3) by detection with a superconducting bolometer at the opposite face.

In a point contact between a metal surface and a metal whisker the conduction electrons accelerated over the contact by an applied voltage V spontaneously emit phonons up to frequencies eV/h. The resulting mode population as a function of energy ε is according to $(eV-\varepsilon)/\varepsilon l_{ph}$, where l_{ph} is the phonon mean free path, but of course constrained to the maximum phonon energy in the metal [2]. In the present experiment the contacts were made of a Au film (thickness ~500 Å, maximum phonon energy ~150 cm^{-1}), evaporated onto the surface of the crystal, and a Au whisker pressed to the film. A good fraction of the phonons generated by the point contact is injected into the crystal over an area with a typical diameter equal to the thickness of the layer. Note here that the phonon time of flight across the film is of the order 10^{-11} s, and that the frequency distribution of the phonons will already be modified to some extent upon their arrival at the hot area due to their finite mean free path in the metal. Adopting at this point an effective temperature of the phonons, and equilibrating the electrical power to the phonon energy traversing the metal–crystal interface per second, we find an effective temperature over the hot area of $T_{eff} \sim 500$ K at 0.1 W. Further thermalization is expected to take place directly following injection into the Al_2O_3 crystal, as from thermal conductivity measurements the mean free path in Al_2O_3 is known to be shorter than the hot-area diameter at the relevant temperatures [3]. We will assume, in an admittedly simplified model, that the phonons will leave the area of generation with a frequency distribution according to $p(\omega, T)D(\omega)$, where $p(\omega, T) = [\exp(\hbar\omega/k_B T_{eff}) - 1]^{-1}$ is the phonon occupation number, and $D(\omega)$ is the density of phonon states of the ruby. During the subsequent ballistic flight no modification of this distribution is anticipated.

With a superconducting Sn bolometer, which

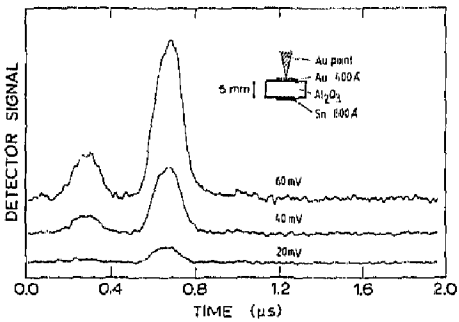

Fig. 1. Time of flight of phonons generated by a Au–Au point contact in a sapphire crystal (Al_2O_3) at 1.2 K with broadband detection. The resistance of the point contact is 5 Ω. The superconducting Sn bolometer is operated at the critical magnetic field.

essentially is a broadband detector, we observed the phonons generated in the point contact to ballistically traverse a sapphire crystal of 5 mm length along the c axis. In fig. 1 we have plotted the phonon signal versus time of arrival for various voltages of the pulse applied to the contact. The pulse width was 170 ns. Two peaks are observed representing the arrival of the longitudinal and the two degenerate transverse modes. The arrival times measured agree with the known sound velocities of these modes in the Debye limit, 11^4 m/s for the longitudinal modes and 6×10^3 m/s for the transverse ones [4]. The phonon signal of both branches is further found to be linear with electrical power up to 2.5 mW over a range of resistances of the point contact.

In a ruby crystal the fluorescent Cr^{3+} ions provide a frequency-selective detection of the phonon occupation numbers in the following way. After population of the $\bar{E}(^2E)$ excited state by optical pumping, the phonon-assisted transitions lift the ions to $\overline{2A}(^2E)$ 29 cm^{-1} above $\bar{E}(^2E)$. The associated increase of the R_2 luminescence thus is a direct measure of the incident phonon occupation. The scheme is well-known to be sensitive to 29 cm^{-1} phonons by the direct absorption $\bar{E}\rightarrow\overline{2A}$ [5]. It has recently been realized [6, 7], however, that very-high-frequency phonons, when sufficiently abundant, invoke by Raman processes a signal that eclipses that of the 29 cm^{-1} phonons. The Raman associated signal ΔR_2 integrated over the spectrum amounts to $\Delta R_2 \sim R_1 \Delta t/T_{\mathrm{Ram}}$, where Δt is the width of the voltage pulse and

$$1/T_{\mathrm{Ram}} = C\int \mathrm{d}\omega (k^2 k_1^2/\omega\omega_1) p(\omega) D(\omega) D(\omega_1), \quad (1)$$

where $p(\omega)D(\omega)$ is the number of incident phonons with frequency between ω and $\omega+\mathrm{d}\omega$, k is the wavevector, $D(\omega)$ is the density of states, and C is a known prefactor; ω_1 and k_1 refer to the outgoing phonon, which has an energy diminished by 29 cm^{-1}. The frequency selectivity of the detection thus is provided by $(k^2k_1^2/\omega\omega_1)D(\omega_1)$, which clearly favors the zone boundary. From similar considerations for the direct process we note that the 29 cm^{-1}-phonon-induced ΔR_2 takes over for effective temperatures only below 30 K.

In fig. 2 the R_2 intensity induced by a pulsed point contact is shown for various distances between a Au–Au point contact and the detection volume (cylinder 50 μm in diameter and 100 μm in length) and a fairly high pulse power (70 mW). The detection volume was prepared by optical

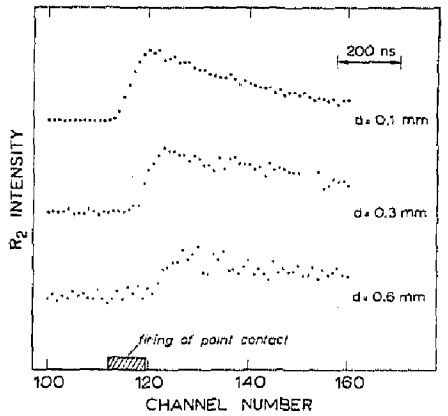

Fig. 2. R_2 intensity induced by a Au–Au point contact at various distances d from the contact at 1.5 K. The resistance of the point contact is 0.5 Ω. Horizontal axis represents time.

pumping with an Ar laser into the broad bands and further selected by the optical imaging system. The phonons produced in the non-radiative decay to $\bar{E}$ give rise to an unwanted R_2 background signal, which in an actual experiment was removed by switching off the pumping a few μs prior to the firing of the point contact. This allows the R_2 background to decay, thus reducing the noise. The sensitivity, on the other hand, is fully retained as the $\bar{E}$ population decays on the time scale of τ_R (~4 ms). In fig. 2, from the shift in arrival time versus distance the velocity is found to be about half the Debye velocity, indicative of detection of near-zone-boundary phonons at the higher applied voltages. Fig. 2 also demonstrates that use of point contacts combined with optical detection makes possible time of flight experiments over submillimeter distances, which are essential in case of near-zone-boundary phonons because of the small group velocity and limited lifetime. The technique further permits a precise and flexible control of the generator-detector configuration. For lateral displacement this is shown in fig. 3, where advantage is taken of scanning of the detection volume along the laser beam by the optics.

To better demonstrate that the point contact is capable of generating phonons near the zone boundary that are detected by Raman processes in the optical detector, we have measured the phonon-induced R_2 intensity versus power P dissipated in the point contact. The generator-detector distance here is 0.1 mm. It appears that above $P = 3$ mW ΔR_2 rises linearly. This corresponds with the classical limit, i.e., $k_B T$ is larger than all $\hbar\omega$ of the system. At lower powers a $P^{1.7}$ dependence is observed, which is indeed consistent with a point contact acting as a Planck's radiator ($P \propto T_{\text{eff}}^4$) and detection by Raman processes ($T_{\text{Ram}}^{-1} \propto T_{\text{eff}}^7$), yielding an exponent 7/4 upon eliminating T_{eff}. For a more quantitative treatment, we have worked out the model of phonon generation by the point contact described above to obtain T_{eff} versus P (fig. 4).

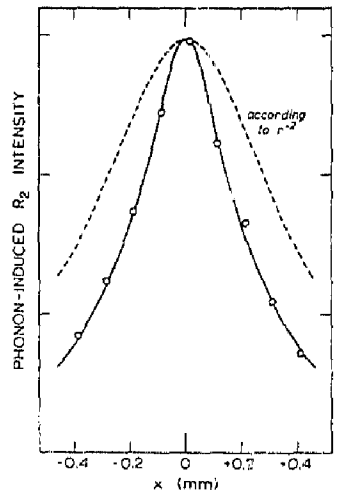

Fig. 3. R_2 intensity vs. the lateral displacement x along the laser beam at a distance $d = 0.4$ mm from the point contact. Dashed curve is the fall with x according to r^{-2}, with $r^2 = d^2 + x^2$.

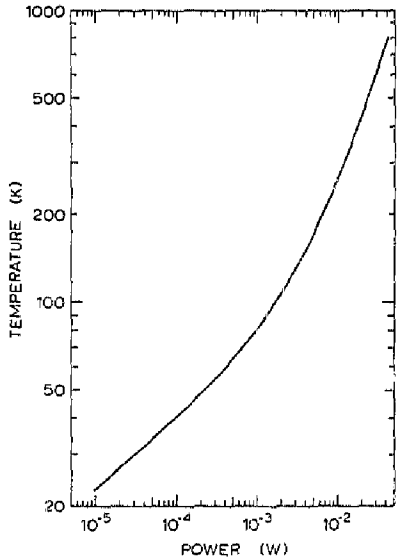

Fig. 4. Effective temperature of the point-contact phonon generator vs. electrical power according to the model described in the text.

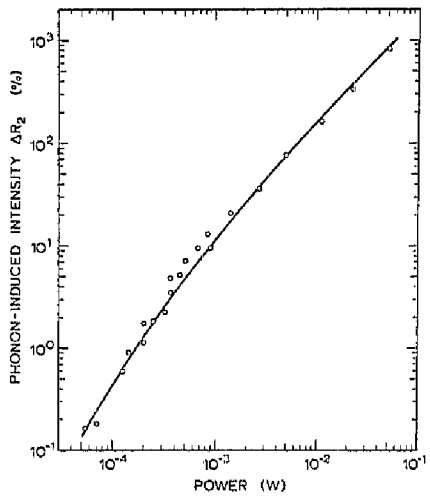

Fig. 5. R_2 intensity vs. electrical power applied to the point contact at 1.5 K. The phonon-induced R_2 signal is normalized to R_1 due to stationary optical pumping ($R_2/R_1 \sim 4\times 10^{-5}$). The volume of detection is a cylinder of 50 μm diameter and 100 μm length. The curve represents the results of the model calculations.

Here, the hot area bordering the ruby was taken to have a diameter 500Å. Combining this with eq. (1) with due account for the overall reduction of the phonon energy density with distance of travel, we see that the simplified model adopted (solid line in fig. 5) excellently tracks the data, both functionally and in absolute magnitude. We emphasize that the model does not involve any adjustable parameters, but we note that we have made minor scaling corrections, within the uncertainties, in the above values for the hot area size and the generator-detector distance. In fig. 5 the effective temperatures of the hot spot range from 30 K to 600 K.

In summary, the present experiments have demonstrated that (a) point contacts are efficient generators for phonons with energies up to the zone boundary in crystals such as Al_2O_3, (b) the use of point contacts enables one to perform time of flight experiments at both small distances and angular resolution, and (c) very-high-frequency phonons travel over macroscopic distances.

References

[1] I.K. Yanson, Zh. Eksp. Teor. Fiz. 66 (1974) 1035.
[2] A.G.M. Jansen, A.P. van Gelder and P. Wyder, J. Phys. C13 (1980) 6073.
[3] R. Berman, Adv. Phys. 2 (1953) 103.
[4] B. Taylor, H.J. Maris and C. Elbaum, Phys. Rev. B3 (1971) 1462.
[5] K.F. Renk and J. Deisenhofer, Phys. Rev. Lett. 26 (1971) 764.
[6] J.G.M. van Miltenburg, J.I. Dijkhuis and H.W. de Wijn, to be published.
[7] R.J.G. Goossens, J.I. Dijkhuis and H.W. de Wijn, to be published.